| | |
|---|---|
| Title | Color-tunable and Phosphor-free White-light Multi-layered Light-emitting Diodes |
| Author(s) | CHEUNG, YF; Choi, HW |
| Citation | IEEE Transactions on Electron Devices, 2013, v. 60, p. 333 |
| Issued Date | 2013 |
| URL | http://hdl.handle.net/10722/189019 |
| Rights | Creative Commons: Attribution 3.0 Hong Kong License |

# Color-Tunable and Phosphor-Free White-Light Multilayered Light-Emitting Diodes

Y. F. Cheung and H. W. Choi, *Senior Member, IEEE*

***Abstract*—A tightly integrated 3-D RGB light-emitting diode (LED) stack is demonstrated. Chips of identical dimensions are stacked on top of each other, with wire bonds embedded within. This is achieved by integrating laser-micromachined channels onto the sapphire face of InGaN LEDs, serving to accommodate wire bonds from the chip beneath. The resultant structure eliminates leakage of monochromatic light from individual chips, producing optimally mixed emission through the top aperture. The device can emit a wide range of colors and is an efficient phosphor-free white-light LED as well. When emitting at correlated color temperatures (CCTs) of 2362 K, 5999 K, and 7332 K, the device generates ∼20 lm/W, exhibiting performance invariant of CCT. Thermal characteristics of this multilayered device are investigated via infrared thermometry.**

***Index Terms*—Color tuning, light-emitting diode (LED).**

## I. Introduction

AN INCANDESCENT lamp's color temperature changes with the temperature of the tungsten element, although the emission remains broadband throughout. Fluorescent lighting emits with fixed spectral characteristics. To generate different colors from such light sources, filters are used to remove the unwanted spectral components, incurring energy losses. Light-emitting diodes (LEDs), on the other hand, produce monochromatic radiation by nature; by mixing the emissions from multiple LEDs, a wide range of colors across the visible spectrum can be obtained. Solutions based on this concept, in the form of RGB LEDs whereby chips emitting the primary colors are bonded onto the same package adjacent to each other, are now available and have been adopted on LED panel displays [1]. The technological progresses of blue-light-emitting InGaN quantum well (QW) and red-light-emitting AlInGaP QW LEDs have resulted in promising device characteristics [2]. However, the strong charge separation in InGaN QWs results in low internal quantum efficiencies at longer wavelengths (high In concentration); fortunately, several methods have been pursued to suppress this effect [3]–[6]. Apart from relying on AlInGaP, several recent approaches have been proposed to achieve red-light-emitting LEDs based on III-nitride technology [7]–[9]. Such developments make RGB emitters more promising than ever. Nevertheless, a major drawback of this approach is the spatial color variations giving rise to nonideal color mixing as emission cones from the discrete devices do not overlap with each other completely [10]. Consequently, the dimensions of chips in RGB LEDs are typically kept small ($< 500\ \mu$m), which also set limitations on the overall output power that can be delivered. Additionally, diffusers are often used to overcome this problem, although optical losses of ∼20% are inevitable [11], together with a loss of color sharpness and richness. In view of such limitations, the stacked LED architecture has been proposed, whereby RGB LED chips are physically stacked on top of each other. The light paths of the three devices become aligned to each other, producing broad-band emission that is naturally mixed without additional optics. The rationale for adopting this design has been explained in [12] and [13].

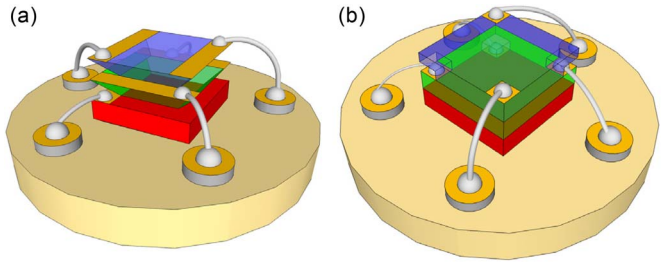


Fig. 1. Schematic diagrams depicting the (a) originally proposed stacked LED with truncated pyramidal chips and (b) the present version with embedded wire bonds.

A major challenge with this design is the accommodation of wire bonds to the LED chips. The original design makes use of chips of truncated pyramidal geometry [14] so that, when stacked together, the bonding pad regions remain exposed, as shown in Fig. 1(a). In reality, despite significant improvements to color homogeneity, leakage of monochromatic light around the pad regions remains severe. It is apparent that, in order to solve the problem completely, chips in a stack have to be of identical dimensions to overlap with each other completely. In this paper, a new chip stacking architecture is demonstrated, overcoming the limitations described before. The RGB chips are of identical dimensions, eliminating possibilities of optical leakage. This is achieved by forming channels onto the sapphire substrates by laser micromachining [15], designed to snug fit the wire bonds. When assembled, the bond wires would appear to protrude from the stacked chip tower, while the tower maintains a planar facet. Fig. 1(b) shows a schematic diagram of the updated design.

Manuscript received September 19, 2012; revised November 9, 2012; accepted November 14, 2012. Date of publication December 7, 2012; date of current version December 19, 2012. This work was supported by a General Research Fund of the Research Grant Council of Hong Kong (Project HKU 7117/11E). The review of this paper was arranged by Editor J. Huang.

The authors are with the Department of Electrical and Electronic Engineering, The University of Hong Kong, Hong Kong, Hong Kong (e-mail: yfcheung@eee.hku.hk; hwchoi@hku.hk).

Color versions of one or more of the figures in this paper are available online at http://ieeexplore.ieee.org.

Digital Object Identifier 10.1109/TED.2012.2228866

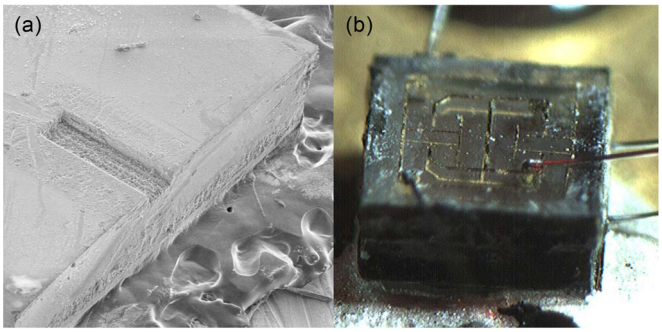


Fig. 2. (a) SEM image showing a laser-micromachined channel on the backside sapphire face of a 1-mm$^2$ InGaN LED chip. (b) Optical microphotograph showing an assembled LED stack.

## II. Experimental Details

The red, green, and blue LED chips used in this study emit with center wavelengths of 640, 510, and 470 nm, respectively, fabricated from metal–organic chemical vapor deposition (MOCVD)-grown AlInGaP on GaAs and InGaN on sapphire wafers. The sapphire substrates of the nitride wafers have been thinned down to $\sim$150 $\mu$m, followed by the fabrication of devices via standard microfabrication processes, subsequently diced into 1-mm$^2$ chips by laser micromachining using a nanosecond diode-pumped solid-state ultraviolet (349 nm) laser source. Channels are formed at the locations of wire bonds of the chip beneath; they are micromachined with the same laser as used for dicing. The chips to be machined are placed on an $x-y$ motorized platform with the sapphire surface facing up. The laser beam, expanded and collimated by a beam expander, trepans across the surface to form a 2-D channel of desired dimensions. Fig. 2(a) shows a SEM image of one such channel formed on the backside sapphire face of a LED chip.

The stack assembly begins with adhering the bottom n-contact of a red AlInGaP vertical LED chip onto a TO-can using electrically conductive epoxy; the top p-electrode is wire bonded to a lead on the TO-can. The green InGaN LED chip with laser-micromachined bottom channel is aligned to cover the red LED in its entirety and so that the wire bonds of the red LED fit snugly into the trench; in fact, this snap-in action automatically aligns the chips. Between chips, optical epoxy is applied to secure them in position. The p-electrodes on the green LED are then wire bonded to the package. Similarly, the blue InGaN LED chip is piled on top of the green LED, forming a trilayer tower structure, as illustrated in the optical microphotograph of Fig. 2(b). The optical measurements are performed by mounting the packaged LEDs onto the input port of a 2-in integrating sphere, fiber coupled to a radiametrically calibrated optical spectrometer. The junction temperatures of the LED chips are determined from infrared thermometry, imaged with a calibrated long-wave infrared (LWIR) camera (FLIR SC645) with a resolution of 640 $\times$ 480.

## III. Results and Discussions

The color homogeneity of the stacked device is evaluated, being the primary goal of this design. The red, green, and blue chips in a stack are biased at currents of 79, 109, and

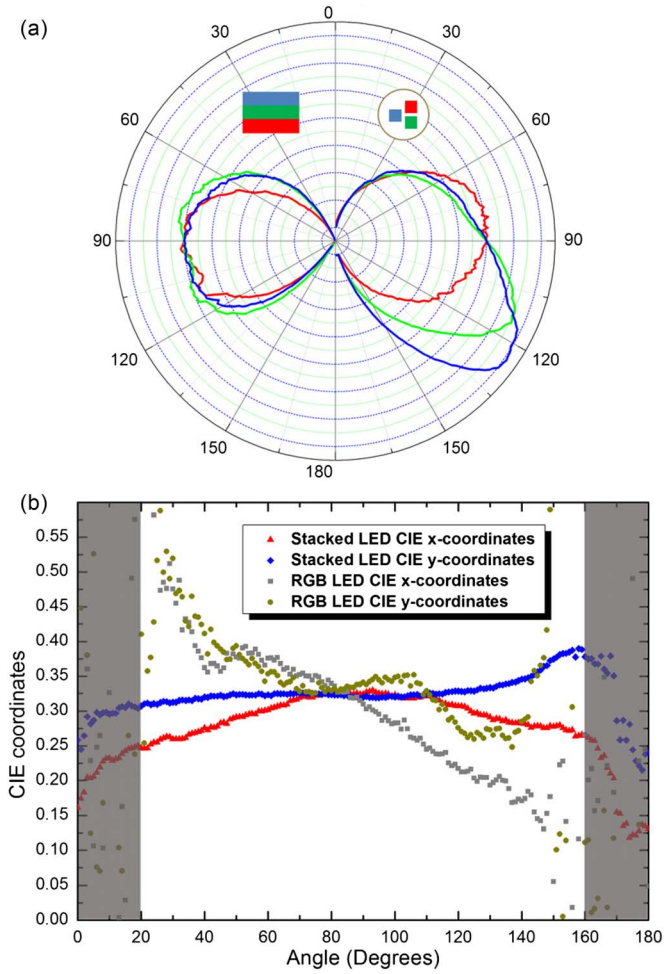


Fig. 3. (a) Polar emission plots for the red, green, and blue spectral components of the (left) stacked LED and the (right) commercial RGB LED. (b) Plot of CIE $x, y$ coordinates versus detection angle for the stacked and planar RGB devices.

38 mA in order to emit white light with CIE coordinates of (0.3, 0.3) when measured in the normal direction. The measurement of angular emission profiles is one of the methodologies for assessing color homogeneity. For comparison, the same set of measurements is performed on a commercial RGB LED (Avago ASMT-QTC0-0AA02). An optical fiber, coupled to a spectrometer, is rotated about the central axis of the device being tested. The blue, green, and red chips in the stack tower are turned on sequentially, with the optical intensity at each angle between 0° and 180° in steps of 1° recorded (90° being the normal direction). The data collected from the stacked LED are plotted onto the left hemisphere of the polar graph, as shown in Fig. 3(a), while the right hemisphere shows the data from the conventional RGB LED. The shapes of the angular plots are self-explanatory: The emission graphs of the stacked tower overlap with each other, as if they are emitted from the same chip. On the other hand, the emission from individual chips in the conventional RGB LED exhibits distinct directionality, giving rise to an overall nonhomogeneous appearance. To investigate the variation of CIE coordinates with respect to viewing angles between 0° and 180° (90° being the normal direction), all three chips in the stacked tower are turned on simultaneously

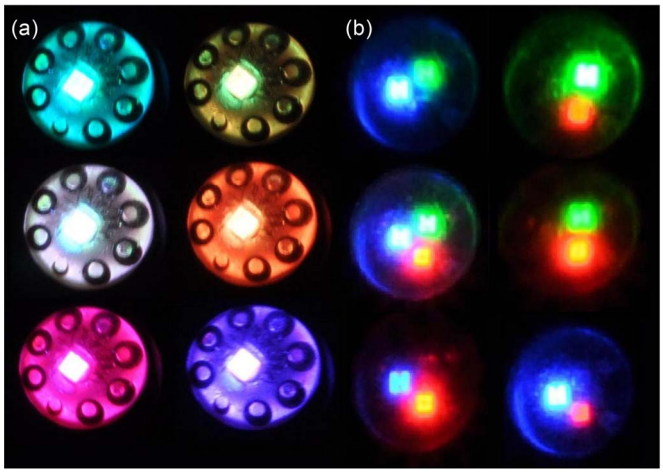


Fig. 4. Optical microphotographs showing the (a) stacked LED and (b) planar RGB LED emitting different colors, highlighting the effectiveness of color mixing via chip stacking.

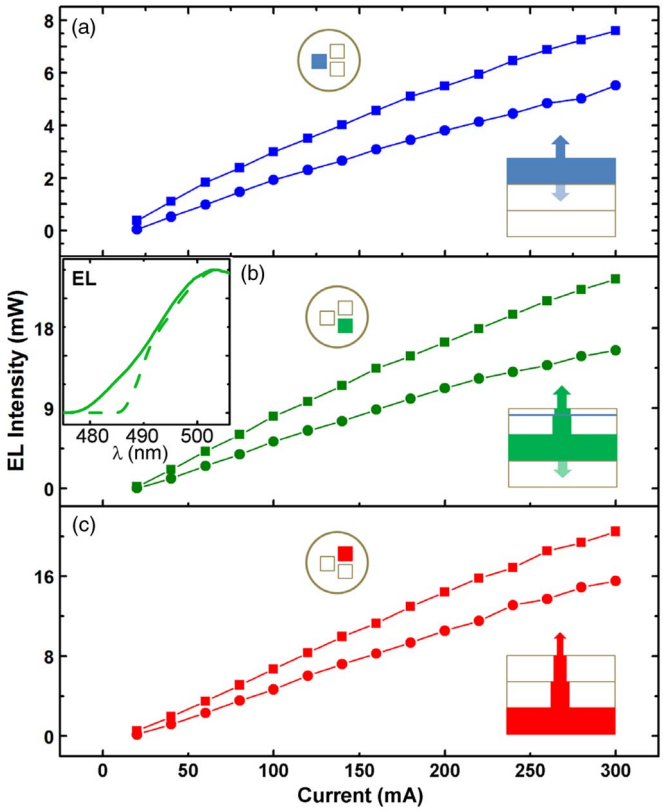


Fig. 5. $L-I$ characteristics of (a) blue, (b) green, and (c) red LEDs in (circle symbols) a stack and in (square symbols) a planar configuration. The plot in the inset of (b) shows the optical EL spectrum of the green LEDs in (dotted line) a stack and in (continuous line) the planar configuration.

under the same testing conditions as before. The CIE $x, y$ coordinates at each angle are plotted against the angle at which the measurement was conducted, as shown in Fig. 3(b). The set of data measured from the conventional RGB LED is plotted onto the same graph.

The CIE coordinates remain relatively unchanged with fluctuations of less than 20% for the stacked tower except for angles below 2° and beyond 160°. Conversely, the CIE coordinates for the conventional RGB LED fluctuate by over 80% across

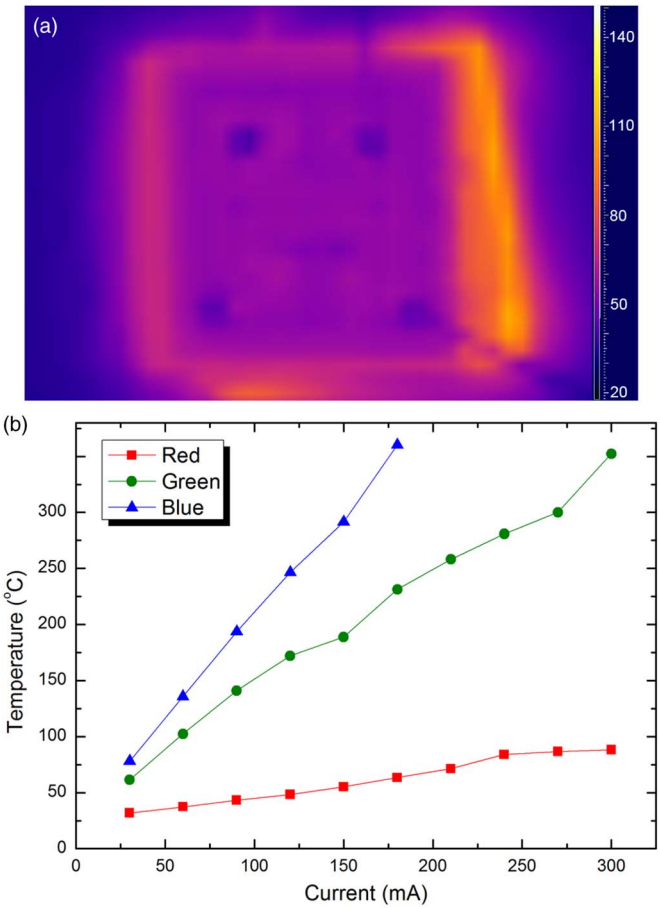


Fig. 6. (a) LWIR image showing an intentionally misaligned RGB stack with the green chip turned on at a current of 60 mA. The surface temperatures are determined from the temperature reading at the edges of the extruded chip. In this case, the average temperature is determined to be ~90 °C.

the same angular range. For both types of devices, the CIE coordinates deviate significantly below 20° and above 160°; this is attributed to the geometries of the packages. The headers on the TO-can block light at wider angles. For the RGB package, the chips are mounted into a recessed cavity so that light is not emitted at wider angles.

While the quantitative measurements presented should be convincing enough, the visual appearances of emission from the devices paint an even clearer picture. Fig. 4(a) and (b) shows the optical photographs of the stacked LED and the conventional RGB LED, respectively, captured in the normal direction using a color CCD camera. Both devices are biased to emit a range of different polychromatic colors by mixing appropriate proportions of red, green, and blue light. Emission from the stacked tower always appears as a single color, a visual proof of satisfactory internal color mixing. On the other hand, red, green, and blue spots of light remain clearly visible from the RGB LED. Note that the linear dimensions of chips in the commercial RGB LED are approximately half of those in the stack. If larger chips are used, the nonhomogeneity would be even more pronounced.

To understand the consequences of stacking to optical performances, $L-I$ characteristics of the chips on different layers of the stack are measured. For the LED chips in the stack, only one of the three chips is turned on for each set of measurements. For

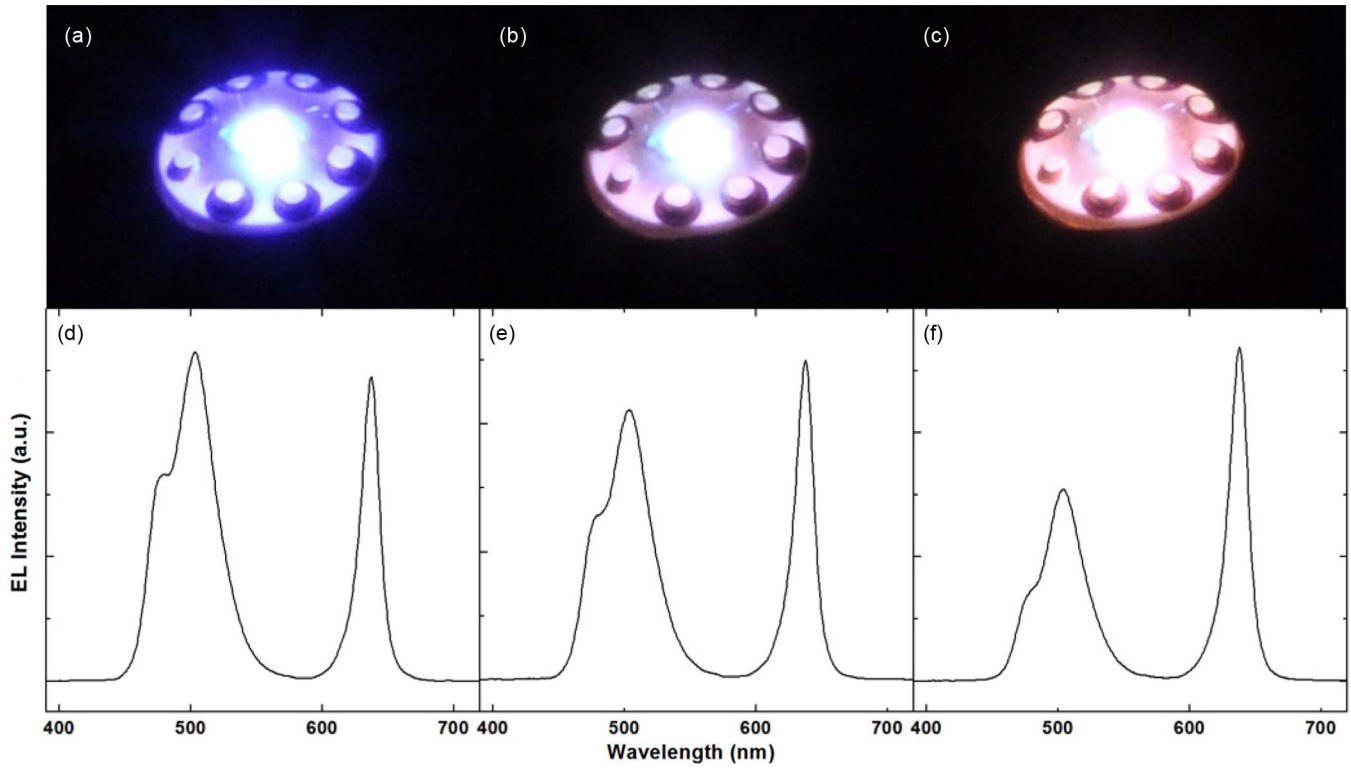


Fig. 7. Optical microphotographs of the stacked LED functioning as a phosphor-free white LED emitting at (a) cool, (b) neutral, and (c) warm white. The corresponding spectra are plotted in (d–f).

a fair comparison, identical RGB chips are mounted side by side onto an identical package, equivalent to the conventional planar RGB LED configuration; the corresponding chip is turned on and measured. The measured $L-I$ data for the blue, green, and red devices are plotted in Fig. 5(a)–(c); the curves formed by square symbols represent data points for the planar RGB devices, while those with circular symbols represent the stacked devices.

At all measured currents, the emitted light intensity by LED chips mounted in a planar configuration is higher than that of the chips integrated into the stacked structure, although to varying extents, due to a combination of thermal, absorption, and reflection effects. For the red LED at the lowest layer of the stack structure, the emitted power drops by ∼24% at 300 mA; this is mainly attributed to interface reflections with minimal thermal effects. Fig. 6(a) shows an LWIR image of an intentionally misaligned RGB stack so that a small portion of the red and green chips are exposed for thermometric measurements. Since the junction is in close proximity to the top surface, the temperature readings obtained from the LWIR image accurately represent junction temperatures. In this figure, the green chip is biased at 60 mA, and the surface temperature reading taken near the edge of the protruded chip is ∼90 °C. Following the same methodology, the surface temperatures of the red, green, and blue chips in the stack at bias currents of 30–300 mA are obtained and plotted in Fig. 6(b), except when the temperature exceeds ∼350 °C. As expected, thermal effects on the red LED are minimal since the chip is attached directly to the package with the junction, staying below 60 °C even at 150 mA, signifying sufficient conductive heat sinking. The remaining optical drops are due to optical losses along the red light optical path, mainly in the form of interface reflection losses. Red light, the longest wavelength of the three, will pass through the green and blue QWs, together with the sapphire substrates, with minimal absorption. For the green LED sandwiched between the red and blue LED chips, reduction in optical power is most severe of the three at ∼34% (at 300 mA); thermal effects are more severe as the generated heat has to be channeled away through the red LED chip. The LWIR data indicate that the junction temperature rises to ∼188 °C at 150 mA. Optically, light emitted downward from the green chip is almost entirely absorbed by the red QWs, while upward emitting light encounters interface reflection losses. This is exacerbated by the partial absorption of the green light by the blue QWs from the chip above, due to spectral overlap between the blue and green QWs. This evident from the sharp absorption edge of the EL spectrum measured from the green-in-stack device shown in the inset of Fig. 5(b), compared to the EL spectrum of the green-in-planar device. Fortunately, such losses can easily be avoided by picking blue and green LED chips with a larger separation of central wavelengths. The blue LED, being at the top, suffers an optical drop of ∼27% (at 300 mA). Being at the top of the stack, there are no reflection losses in the upward optical path, but heat sinking is a major issue with this chip. Heat has to be conducted through the green and red chips to the package, accounting for the high junction temperature attained of ∼291 °C (at 150 mA). At such elevated temperatures, device reliability and efficiency (due to droop effect) would be compromised. A suitable heat-sinking strategy must be in place before the devices can be driven at higher currents.

The thermal and optical analyses provide insight on the major optical loss and heat conduction mechanisms so that suitable remedies to the design can be applied. In particular, a dedicated package allowing direct heat sinking from individual chips (via the facets perhaps) should be designed and implemented to suit the thermal characteristics of the stack. Additionally, the absorption of downward propagated light from the blue and green chips may be eliminated by the coating of a wavelength-selective distributed Bragg reflector on the bottoms of the chips, enabling selective reflection and transmission of light.

The stacked tower also functions as a conversion-free white-light LED and, in fact, a correlated color temperature (CCT)-variable white-light LED. Previously, the use of multilateral QWs [16] and multifacet QWs [17] has also been pursued for realizing phosphor-free white LEDs. Fig. 7(a)–(c) shows the stacked LED operated as cool white (CCT of 7332 K, driven at currents of 79, 120, and 45 mA in the order of RGB), neutral white (5999 K at 79, 110, and 38 mA), and warm white (2362 K at 150, 121, and 29 mA) light sources, respectively, while their corresponding optical spectra are plotted in Fig. 7(d)–(f), respectively. The luminous efficacies of the device operated at the three stated CCTs are 19.23, 20.19, and 20.70 lm/W, respectively, being respectable figures for a prototypic device. For comparison, the planar RGB LED assembled using identical chips performs as follows: 32.02, 32.78, and 37.22 lm/W at CCTs of 7141 K, 6104 K, and 2401 K, respectively. In other words, the efficacy of the stacked LED is approximately 38% lower than its planar counterpart; however, the additional functionalities far overweigh such losses. Mostly importantly, such deficiencies are mainly due to the lack of a suitable package for such architecture, and performances are expected to improve significantly when a solution has been developed. It is also worth noting that the luminous efficacy is nearly independent of CCT, allowing efficient operation at low CCTs, a desirable color for indoor lighting; such characteristics are obviously superior to that of phosphor-converted white LEDs at low CCT due to the low efficiencies of longer wavelength phosphors.

In Fig. 8, the optical performances of the stacked LED functioning as a neutral white LED over a period of 200 s are plotted. The neutral white LED is operated under conditions described in the previous paragraph. It can be seen that, while the luminous flux stabilizes within 60 s, the color characteristics (in terms of CCT and CIE coordinates) stabilize within 30 s. Subsequently, the stacked white LED delivers stable optical output.

The proposed chip stacking design may offer yet another solution for die stacking in microelectronic devices, an important step forward for continuing improvements in device performance [18]. Three-dimensional die stacking is a common strategy for increasing the packing density of memory chips [19]. Two methods are commonly adopted, including placing chips of increasing smaller sizes on top of each other [20] or the insertion of a dummy spacer in between two layers of identically sized ICs [21]. However, the former practice sets a limit on the usable space, while the latter unnecessarily increases the total thickness of the stack. By applying the proposed approach on stacking IC chips, not only can the aforementioned problems be solved, but also improved isolation among bond wires.

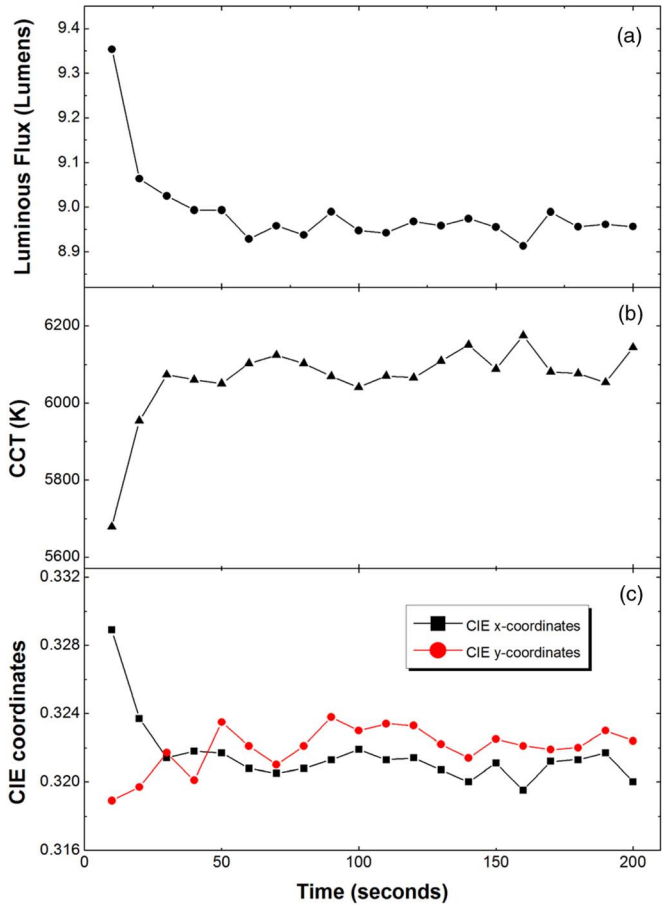


Fig. 8. Luminous flux, CCT, and CIE coordinates of a stacked LED over a period of 200 s. The stacked LED, functioning as a phosphor-free neutral white emitter, is operated at currents of 79, 110, and 38 mA for the RGB chips, respectively.

## IV. Conclusion

The RGB stacked LED architecture has been further optimized to eliminate leakage of monochromatic light from individual chips from each layer, therefore creating a device that functions as both a phosphor-free white-light LED with CCT tuning capabilities and a widely tunable color LED. Through $L-I$ measurements and LWIR thermometry, thermal and optical effects arising from chip stacking have been analyzed, prompting the need for the design of a dedicated package to improve heat dissipation from the chips. The luminous efficacies of the device as a CCT-variable white-light LED are approximately 20 lm/W at CCTs of 7332 K, 5999 K, and 2362 K. With diverse functionalities, the device is suitable for both display and illumination purposes.

## References

[1] N. Shlayan, R. Venkat, P. Ginobbi, and A. K. Singh, "Energy efficient RGBW pixel configuration for light-emitting displays," *J. Display Technol.*, vol. 5, no. 11, pp. 418–424, Nov. 2009.

[2] M. R. Krames, O. B. Shchekin, R. Mueller-Mach, G. O. Mueller, L. Zhou, G. Harbers, and M. G. Craford, "Status and future of high-power light-emitting diodes for solid-state lighting," *J. Display Technol.*, vol. 3, no. 2, pp. 160–175, Jun. 2007.

[3] H. Zhao, G. Liu, J. Zhang, J. D. Poplawsky, V. Dierolf, and N. Tansu, "Approaches for high internal quantum efficiency green InGaN light-emitting diodes with large overlap quantum wells," *Opt. Exp.*, vol. 19, no. S4, pp. A991–A1 007, Jul. 2011.

[4] R. A. Arif, H. Zhao, Y.-K. Ee, and N. Tansu, "Spontaneous emission and characteristics of staggered InGaN quantum-well light-emitting diodes," *IEEE J. Quantum Electron.*, vol. 44, no. 6, pp. 573–580, Jun. 2008.
[5] C. Wetzel and T. Detchprohm, "Wavelength-stable rare earth-free green light-emitting diodes for energy efficiency," *Opt. Exp.*, vol. 19, no. S4, pp. A962–A971, Jul. 2011.
[6] I. L. Koslow, M. T. Hardy, P. S. Hsu, P.-Y. Dang, F. Wu, A. Romanov, Y.-R. Wu, E. C. Young, S. Nakamura, J. S. Speck, and S. P. DenBaars, "Performance and polarization effects in (112) long wavelength light emitting diodes grown on stress relaxed InGaN buffer layers," *Appl. Phys. Lett.*, vol. 101, no. 12, pp. 121106-1–121106-4, Sep. 2012.
[7] J. Zhang and N. Tansu, "Improvement in spontaneous emission rates for InGaN quantum wells on ternary InGaN substrate for light-emitting diodes," *J. Appl. Phys.*, vol. 110, no. 11, pp. 113110-1–113110-5, Dec. 2011.
[8] H. Zhao, G. Liu, and N. Tansu, "Analysis of InGaN-delta-InN quantum wells for light-emitting diodes," *Appl. Phys. Lett.*, vol. 97, no. 13, pp. 131114-1–131114-3, Sep. 2010.
[9] T. K. Sharma and E. Towe, "On ternary nitride substrates for visible semiconductor light-emitters," *Appl. Phys. Lett.*, vol. 96, no. 19, pp. 191105-1–191105-3, May 2010.
[10] H. Wu, N. Narendran, Y. Gu, and A. Bierman, "Improving the performance of mixed-color white LED systems by using scattered photon extraction technique," in *Proc. SPIE*, 2007, vol. 6669, p. 666 905.
[11] C.-C. Sun, W.-T. Chien, I. Moreno, C. T. Hsieh, M.-C. Lin, S.-L. Hsiao, and X.-H. Lee, "Calculating model of light transmission efficiency of diffusers attached to a lighting cavity," *Opt. Exp.*, vol. 18, no. 6, pp. 6137–6148, Mar. 2010.
[12] K. N. Hui, X. H. Wang, Z. L. Li, P. T. Lai, and H. W. Choi, "Design of vertically-stacked polychromatic light-emitting diodes," *Opt. Exp.*, vol. 17, no. 12, pp. 9873–9878, Jun. 2009.
[13] H. W. Choi, K. N. Hui, and X. Wang, "Semiconductor Color-Tunable Broadband Light Sources And Full-Color Microdisplays," U.S. Patent 7 982 228, Jul. 19, 2011.
[14] W. Y. Fu, K. N. Hui, X. H. Wang, K. K. Y. Wong, P. T. Lai, and H. W. Choi, "Geometrical shaping of InGaN light-emitting diodes by laser micromachining," *IEEE Photon. Technol. Lett.*, vol. 21, no. 15, pp. 1078–1080, Aug. 2009.
[15] G. Y. Mak, E. Y. Lam, and H. W. Choi, "Liquid-immersion laser micromachining of GaN grown on sapphire," *Appl. Phys. A*, vol. 102, no. 2, pp. 441–447, Feb. 2011.
[16] I.-K. Park, J.-Y. Kim, M.-K. Kwon, C.-Y. Cho, J.-H. Lim, and S.-J. Park, "Phosphor-free white light-emitting diode with laterally distributed multiple quantum wells," *Appl. Phys. Lett.*, vol. 92, no. 9, pp. 091110-1–091110-3, Mar. 2008.
[17] M. Funato, T. Kondou, K. Hayashi, S. Nishiura, M. Ueda, Y. Kawakami, Y. Narukawa, and T. Mukai, "Monolithic polychromatic light-emitting diodes based on InGaN microfacet quantum wells toward tailor-made solid-state lighting," *Appl. Phys. Exp.*, vol. 1, no. 1, p. 011106, Jan. 2008.
[18] P. G. Emma and E. Kursun, "Is 3D chip technology the next growth engine for performance improvement?" *IBM J. Res. Develop.*, vol. 52, no. 6, pp. 541–552, Nov. 2008.
[19] R. S. Patti, "Three-dimensional integrated circuits and the future of system-on-chip designs," *Proc. IEEE*, vol. 94, no. 6, pp. 1214–1224, Jun. 2006.
[20] W. R. Davis, J. Wilson, S. Mick, J. Xu, H. Hua, C. Mineo, A. M. Sule, M. Steer, and P. D. Franzon, "Demystifying 3D ICs: The pros and cons of going vertical," *IEEE Design Test Comput.*, vol. 22, no. 6, pp. 498–510, Nov./Dec. 2005.
[21] A. Horibe, F. Yamada, C. Feger, and J. U. Knickerbocker, "Inter chip fill for 3D chip stack," *Trans. Jpn. Inst. Electron. Packag.*, vol. 2, no. 1, pp. 160–162, 2009.

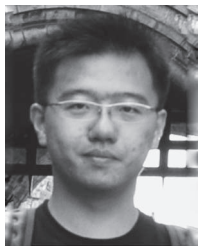

**Y. F. Cheung** received the B.Eng. degree in electronics and communications engineering from The University of Hong Kong, Hong Kong, where he is currently working toward the M.Phil. degree, researching on laser processing on light-emitting diodes.

**H. W. Choi** (SM'09) received the Ph.D. degree from the National University of Singapore, Singapore, in 2003.

In 2004, he joined The University of Hong Kong, Hong Kong, where he is currently an Associate Professor.